CANCER BIOTHERAPY AND RADIOPHARMACEUTICALS
Volume 27, Number 10, 2012

DOI: 10.1089/cbr.2012.1245

Gallic Acid Induces the Apoptosis of Human Osteosarcoma Cells *In Vitro* and *In Vivo* via the Regulation of Mitogen-Activated Protein Kinase Pathways

Cheng-zhen Liang,[1] Xin Zhang,[1] Hao Li,[1] Yi-qing Tao,[1] Li-jiang Tao,[1] Zi-ru Yang,[1] Xiao-peng Zhou,[1] Zhong-li Shi,[2] and Hui-min Tao[1]

Abstract

To examine the antitumor effects of gallic acid (GA) on osteosarcoma, two human osteosarcoma cell lines U-2OS and MNNG/HOS were treated by GA and subjected to cell proliferation and apoptosis assays. In addition, MNNG/HOS xenograft tumors were established in nude BALB/c mice to evaluate the anticancer capacity of GA *in vivo*. The results showed that GA inhibited the proliferation and induced the apoptosis of osteosarcoma cells, accompanied by the upregulation of p-38 activation and the downregulation of c-Jun N-terminal kinase (JNK) and extracellular signal regulated kinase (ERK1/2) activation. Additionally, p38 MAPK inhibitor abrogated GA-induced growth inhibition of osteosarcoma cells, whereas JNK or ERK1/2 inhibitors sensitized osteosarcoma cells to GA-induced growth inhibition. *In vivo* studies further showed that GA administration decreased xenograft tumor growth in a dose-dependent manner. Immunohistochemistry analysis demonstrated the downregulation of PCNA and CD31 expression and upregulation of apoptosis in MNNG/HOS tumor tissues following GA treatment. This study demonstrates the antitumor efficacy of GA for osteosarcoma that is mediated by the modulation of cell proliferation, apoptosis, and angiogenesis. Our findings suggest that GA could be a potent agent for osteosarcoma intervention.

Key words: Apoptosis, Caspase, Gallic acid, MAPK kinases, Osteosarcoma

Introduction

Osteosarcoma, the most common type of malignant bone tumor, occurs predominantly in adolescents and young adults. Osteosarcoma is characterized by frequent metastasis and strong resistance to chemotherapy.[1] This is attributed to a range of matrix elements and growth factors present in the bone microenvironment that establish a vicious crosstalk between cancer and normal bone cells.[2] One potential strategy to overcome chemoresistance of osteosarcoma is to induce apoptosis.[3]

Apoptosis is a form of cell death coordinated by a network of genes and is a key target in the development of new anticancer therapies. Apoptosis can be activated through at least two signaling pathways: caspase dependent and caspase independent.[4] The mitogen-activated protein kinases (MAPKs) are a large family of serine/threonine kinases, which currently include four known MAPKs: the extracellular signal regulated kinase (ERK1/2), the c-Jun N-terminal kinase (JNK), p38, and the big mitogen-activated protein kinase 1 (BMK1).[5] The functions of MAPK signaling in cancer development are complex, and this is consistent with the wide range of cellular responses that they regulate.[6] It is known that activated MAPK signaling might promote cell growth or induce cell death in different situations.[7,8] Several studies have suggested that p38, JNK, and ERK1/2 cascades have a critical role in regulating cytotoxic drug-induced apoptosis in osteosarcoma.[9,10]

Gallic acid (3,4,5-trihydroxybenzoic acid, GA), a major active component of Chinese gall, is widely distributed in

[1]Department of Orthopedics, 2nd Affiliated Hospital, School of Medicine, Zhejiang University, Hangzhou, Zhejiang, People's Republic of China.
[2]Institute of Orthopedic Research, 2nd Affiliated Hospital, School of Medicine, Zhejiang University, Hangzhou, People's Republic of China.

Address correspondence to: Hui-min Tao; Department of Orthopedics, 2nd Affiliated Hospital, School of Medicine, Zhejiang University; #88 Jie Fang Road, Hangzhou, 310009, Zhejiang, People's Republic of China
E-mail: **huimintao_zrgk@163.com**

various natural products, and exhibits a wide variety of biological effects, including antibacterial,[11] antioxidant,[12,13] antifungal and antimalarial,[14] and antiherpetic action.[15] In addition, the antiviral capacity of GA is related to its antioxidant activity.[16] Recently, the antitumor activity of GA has attracted more attention because GA has been shown to be an excellent free radical scavenger and an inducer of differentiation and programmed cell death in a number of tumor cell lines.[8,17–20] Moreover, the *in vitro* antitumor activity of GA against osteosarcoma has been reported by Liao et al.[21] However, in the present study, we aimed to examine the biological effects of GA on osteosarcoma cells *in vitro* and *in vivo* and investigate the underlying mechanism. Our results demonstrated that GA reduced osteosarcoma cell viability through inducing apoptosis *in vitro and in vivo*, and this is attributed to the activation of the p38 signal pathway and the inactivation of the JNK and ERK1/2 MAPK signaling pathways.

Materials and Methods

Cell cultures

The human osteosarcoma cell lines U-2OS (HTB-96TM; ATCC) and MNNG/HOS (CRL-1547TM; ATCC) were obtained from the Cell Bank of Shanghai Institute of Biochemistry and Cell Biology, Chinese Academy of Sciences, where they were tested and authenticated. These procedures include cross species checks, DNA authentication, and quarantine. Cell lines used in the present study were in culture for <6 months. U-2OS were cultured in McCoy's 5a medium supplemented with 10% fetal calf serum (FCS) and 1% penicillin/streptomycin. MNNG/HOS were cultured in Eagle's minimum essential medium supplemented with 10% FCS and 1% penicillin/streptomycin. All the cells were cultured at 37°C in a humidified atmosphere (5% CO_2, 95% air).

MTT and BrdU incorporation assay

The MTT assay was employed to examine the viability of human osteosarcoma cells treated with GA. GA was purchased from Sigma-Aldrich and dissolved in dimethyl sulfoxide (DMSO) as 100 mM stock solution. Briefly, cells were seeded in 96-well plates at $4–8\times10^3$ cells/well in 200 μL medium and cultured for 12 hours to allow attachment. Then, the cells were treated with DMSO (1/1000 diluted in the medium) or various concentrations of GA (0–100 μM) for different periods of time (0–72 hours). Four hours before the end of each incubation period, MTT solution (5 mg/mL in 20 μL PBS; Sigma-Aldrich) was added to each well and incubated for 4 hours at 37°C. The growth medium was then removed and replaced with formazan dissolved in DMSO (150 μL/well). An MR7000 microplate reader (Dynatech) was used to measure the absorbance of each well at 570 nm and IC_{50} values were calculated using the probit model.

Cell proliferation was measured using a cell proliferation enzyme-linked immunosorbent assay (ELISA) kit (Roche Applied Science). After treatment with GA, cells were incubated with 20 μL BrdU labeling solution per well for 4 hours and then dried and fixed, and detected using anti-BrdU mAb according to the manufacturer's instructions. Finally, the absorbance of the samples was measured by a microplate reader at 450 nm.

P38 MAPK inhibitor SB203580 (Cell Signaling), Jun N-terminal kinase (JNK) inhibitor SP600125 (Merck), and ERK inhibitor PD98059 (Sigma-Aldrich) were dissolved in DMSO immediately before use. Cells were pretreated with SB203580 (20 μM for 30 minutes), SP600125 (20 μM for 30 minutes), or PD98059 (30 μM for 30 minutes) before GA was added in the medium. Cells were tested by BrdU incorporation after incubation for 24 hours. The control group was treated with vehicles. The inhibitory rate of cellular proliferation was calculated as $[1–A_{570}(\text{test})/A_{570}(\text{control})]\times100\%$. Data represented the mean of six replicates, each performed in triplicate.

Hoechst staining

Hoechst staining was employed to evaluate the apoptosis of human osteosarcoma cells treated with GA. Briefly, the cells were exposed to GA for 24 hours and then stained with Hoechst 33258 (5–10 μg/mL; Sigma-Aldrich) for 10 minutes. After being washed with phosphate-buffered saline (PBS), they were observed under a fluorescence BX51 microscope (Olympus). Hoechst 33258 freely permeates cell membranes and stains nuclear DNA as blue. Apoptotic cells were identified by the presence of condensed or fragmented nuclei stained either blue or red, depending on apoptotic stage.

Annexin V-FITC/PI double staining

Annexin V-FITC/PI double staining was employed to quantify the apoptosis of human osteosarcoma cells treated with GA. Briefly, cells were seeded in six-well plates at 2×10^5 cells/well and exposed to GA (0–75 μM) for 24 hours. The cells were then stained using annexin V-FITC/PI double-fluorescence apoptosis detection kit (Biouniquer Technology) following the manufacturer's instruction. Samples were analyzed using an FACSCalibur flow cytometer within 1 hour after the staining.

Real-time quantitative RT-polymerase chain reaction analysis

Total RNA was isolated from the cells using Trizol (Invitrogen) according to the manufacturer's instructions. cDNA was generated from total RNA (2 μg) by using 1 μl primer mix [including oligo(dT)18 and random primers], 25 units RNase inhibitor, 2 μL dNTPs (10 mM), and a Moloney Murine Leukemia Virus reverse transcriptase cDNA synthesis kit (Promega). Quantitative real-time polymerase chain reaction (PCR) was performed using Applied Biosystems 7500 Real-Time PCR System and SYBR® Premix Ex Taq™ kit (Perfect Real Time) (TaKaRa). The cycle threshold (CT) values for each gene were corrected using the mean CT value. Real-time PCR data were quantified using the ΔCT method with the formula: $n=100\times2^{-(\Delta\text{CT targeted gene}-\Delta\text{CT 18s rRNA})}$. The primers used were 18 seconds rRNA: forward 5′GACTCAACACGGGAAACCTCAC3′ and reverse 5′CCAGACAAATCGCTCCACCAAC3′; ERK1/2: forward 5′ GCTTTTCCCCAAGTCAGACTCCAA3′, reverse 5′ CTCATCCGTCGGGTCATAGTACT3′; JNK: forward 5′CCATCATCATCGTCGTCTGTCAATG3′ and reverse 5′CTGCTTCTAGACTGCTGTCTGTATC3′; p-38: forward 5′CCTTCAGGAGAATCTACACGCATGT3′ and reverse 5′ TGGAGAGTGCAGTAGCCAGAAGA3′.

Caspase enzyme activity assay

To examine whether the apoptotic effects induced by GA were associated with caspase enzyme activation or not, the activities of initiator caspase (caspase-8 and -9) and effector caspase (caspase-3) were investigated. A total of 0.8×10^4 cells were seeded per well on a 96-well plate. After 24 hours of incubation, different concentrations (0–75 μM) of GA were added in different groups. Then, caspase-3, -8, and -9 enzyme activity was measured using the caspase-Glo ratio colorimetric analysis kit (Promega). The absorbance values were determined at 405 nm wave length. The assays were performed in triplicate using various sample dilutions.

Immunoblotting

Briefly, cells were washed twice with ice-cold PBS; resuspended in 200 μL ice-cold solubilizing buffer containing 300 mM NaCl, 50 mM Tris-HCl (pH 7.6), 0.5% Triton X-100, 2 mM phenyl-methanesulfonyl fluoride (PMSF), 2 μL/mL aprotinin, and 2 μL/mL leupeptin; and incubated at 4°C for 1 hour. Lysates were collected after centrifuging at 13,000 rpm for 20 minutes at 4°C. Protein levels were quantified using a BCA protein assay kit (Pierce) according to the manufacturer's instruction. Equivalent amounts of protein were separated by 8%–12% sodium dodecyl sulfate–polyacrylamide gel electrophoresis and transferred to polyvinylidene fluoride membranes. The membranes were blocked in PBS containing 5% nonfat dry milk (w/v), and then incubated overnight at 4°C with antibodies against ERK1/2, phosphor-ERK1/2 (p- ERK1/2), p38, phosphor-p38 (p-p38), JNK, and phosphor-JNK (p-JNK) (Cell Signaling Technology) at the recommended dilutions. The membranes were then incubated with HRP-conjugated goat anti-mouse secondary antibodies (Cell Signaling Technology) at room temperature for 1 hour, and developed using the enhanced chemiluminescence reagents (Cell Signaling Technology) and exposed to X-ray film.

Xenograft model

Female BALB/c (*nu/nu*) mice (weight 16–18 g) were obtained from the Shanghai Pharmaceutical Institute of Academy of Science (Shanghai), and maintained under specific pathogen-free conditions and supplied with sterile food and water *ad libitum*. Approximately 5×10^6 MNNG/HOS cells were injected subcutaneously into the right axillary fossa of each nude mouse under aseptic conditions as described previously.[22] The next day (day 1) mice were randomly divided into three groups ($n=6$) and fed plain drinking water (control), or 0.3% and 1% GA w/v in drinking water. Diet and water consumption as well as animal body weight were monitored regularly throughout the study. Once xenograft started growing, their sizes were measured in two dimensions using digital vernier calipers. The tumor volume was calculated by the following formula: $0.5\times a\times b^2$, where "a" was the largest dimension and "b" was the perpendicular diameter. Lethal toxicity was defined as any death in treated animals occurring before the first death in the control group. Mortality was monitored daily. At the end of the study period, tumors were excised and fixed in 10% formalin for immunohistochemical analysis. The animal studies were approved by the Ethics Committee of Zhejiang University Medical College and the principles of laboratory animal care were followed in all animal experiments.

Immunostaining

Formaldehyde-fixed, paraffin-embedded tissue blocks were prepared from xenograft tissue and cut into serial sections (3 μm), which were then mounted on glass slides and dried at 60°C for 2 hours. Tissue sections were deparaffinized in xylene, rehydrated, and then immersed in PBS. To block endogenous peroxidase activity, the slides were treated with 3% H_2O_2 for 15 minutes, washed with PBS three times (3 minutes each), and immersed in boiling 0.01 M sodium citrate buffer (pH 6.0) for 10 minutes. Next, sections were incubated with goat serum for 30 minutes at room temperature and then with mouse monoclonal antibodies against proliferating cell nuclear antigen PCNA and CD31 (diluted at 1:1,000; Abcam) at 4°C overnight. After washing in PBS for 5 minutes, sections were incubated in biotin-labeled goat anti-rabbit IgG (diluted 1:200) at 37°C for 30 minutes and the secondary antibody was detected by SABC method. Terminal deoxynucleotidyl transferase-mediated nick end labeling (TUNEL) kit (Roche) was used to detect apoptosis in the xenograft tissue according to the manufacturer's instructions.

PCNA-, CD31-, and TUNEL-positive cells were analyzed using the Image Pro-Plus software (ver. 6.0; Media Cybernetics), according to the method developed by Xavier et al.[23] Briefly, a DP 70 CCD camera (Olympus) coupled to an AX-70 microscope (Olympus) was used to capture, at 400× magnification, 10 digital images (resolution 2560×1920 pixels) per slide. Measurement parameters included IOD, total area, and mean density. OD was calibrated and the area of interest assigned values for hue (0–30), saturation (0–255), and intensity (0–220). Images were then converted to grayscale and values were counted.

Statistical analysis

The data were expressed as the mean ± standard deviation (SD). Mean values were calculated from data obtained from experiments performed in triplicate. One-way analysis of variance was used to identify statistically significant differences between the experimental and control groups. IC_{50} values (and 95% confidence intervals) were calculated from MTT assay data by probit regression. The Kruskal–Wallis and Mann–Whitney U tests were used to identify differences in PCNA-, CD31-, and TUNEL-positive expression between different treatment groups.

All statistical analyses were performed using the SPSS software (ver. 16.0; SPSS, Inc.). p-Values were two-tailed and a value <0.05 was considered statistically significant.

Results

GA inhibits the proliferation of human osteosarcoma cells in a dose- and time-dependent manner

To investigate the effects of GA on the proliferation of osteosarcoma cells, we measured the growth of U-2OS and MNNG/HOS cells, using the MTT and BrdU incorporation assays. The results showed that GA inhibited cell proliferation in a dose- and time-dependent manner (Fig. 1). After 24 hours, IC_{50} values for GA were 54.23 μM in U-2OS and

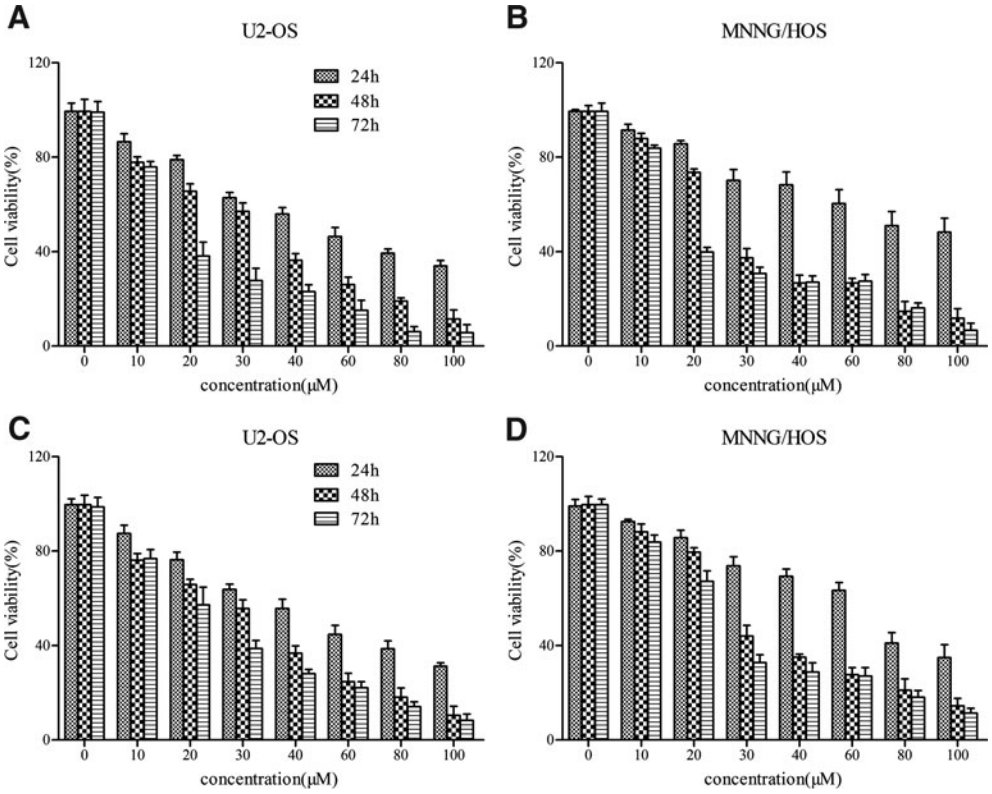

FIG. 1. GA inhibits the proliferation of human osteosarcoma cells in a dose- and time-dependent manner. **(A, B)** Cells were exposed to GA with different concentrations for various time and the OD values were obtained through reading plate at 570 nm with 96-well microtest spectrophotometer by MTT assay. **(C, D)** After exposing to GA with different concentrations for various time, cell proliferation was analyzed by BrdU incorporation assay. The viability rate was expressed as the percentage of cell viability rate compared with the control. The data were expressed as mean ± SD obtained from triplicate samples. GA, gallic acid.

87.12 μM in MNNG/HOS cells according to the MTT assay. Similar IC_{50} values were also calculated according to the BrdU assay (data not shown). Inhibition was not saturated in any of the two osteosarcoma cell lines at the concentrations of GA used.

GA induces the apoptosis of human osteosarcoma cells

To study the mechanism by which GA inhibits the proliferation of human osteosarcoma cells, we performed Hoechst 33258 staining and TEM and FCM analyses. Hoechst 33258 staining showed that U-2OS and MNNG/HOS treated with GA exhibited morphological features of early apoptotic cells (Fig. 2A). Also, the number of late apoptotic cells increased at higher GA concentration in two osteosarcoma cell lines. Maximal cell death occurred within 48 hours of drug exposure (data not shown). Thus, we selected 24-hour exposure to GA as an appropriate time point for subsequent experiments.

TEM showed typical apoptotic morphological features induced by GA: aggregated karyotin, denser cytoplasm, and the formation of dense, round apoptotic bodies (Fig. 2B). These results were consistent with the morphological alterations observed by light and fluorescence microscopy.

Next, we found that the cell cycle progression was not obviously influenced after exposure to GA (data not shown), which was not consistent with other reports.[19,20] However, Annexin V-FITC/PI double staining showed early apoptosis induced by GA in both U-2OS and MNNG/HOS cells. U-2OS and MNNG/HOS cells treated with GA exhibited much higher rates of apoptosis (57.7% and 42.3%) than that of control cells (3.3% and 4.7%) (Fig. 2C). Most apoptotic cells were in the early stages.

Moreover, caspase enzyme activity assay showed that GA caused dose-dependent activation of caspase-3 and -9 by two- to threefolds (Fig. 2D), which agreed with other reports.[24,25] However, there was a negligible increase in caspase-8 activity. Taken together, these findings revealed that GA inhibits the proliferation of human osteosarcoma cells mainly via inducing apoptosis rather than inducing cell necrosis.

GA induces human osteosarcoma cell apoptosis via the inhibition of ERK1/2 and JNK and the activation of p38 kinase signaling

To elucidate the molecular mechanism by which GA induces apoptosis of human osteosarcoma cells, we performed Western blot analysis to examine the signaling pathways involved. The results showed that the levels of p-JNK and p-ERK1/2 kinase decreased significantly after the treatment with GA, while the level of p-p38 kinase increased significantly (Fig. 3A). In addition, the changes in the levels of these

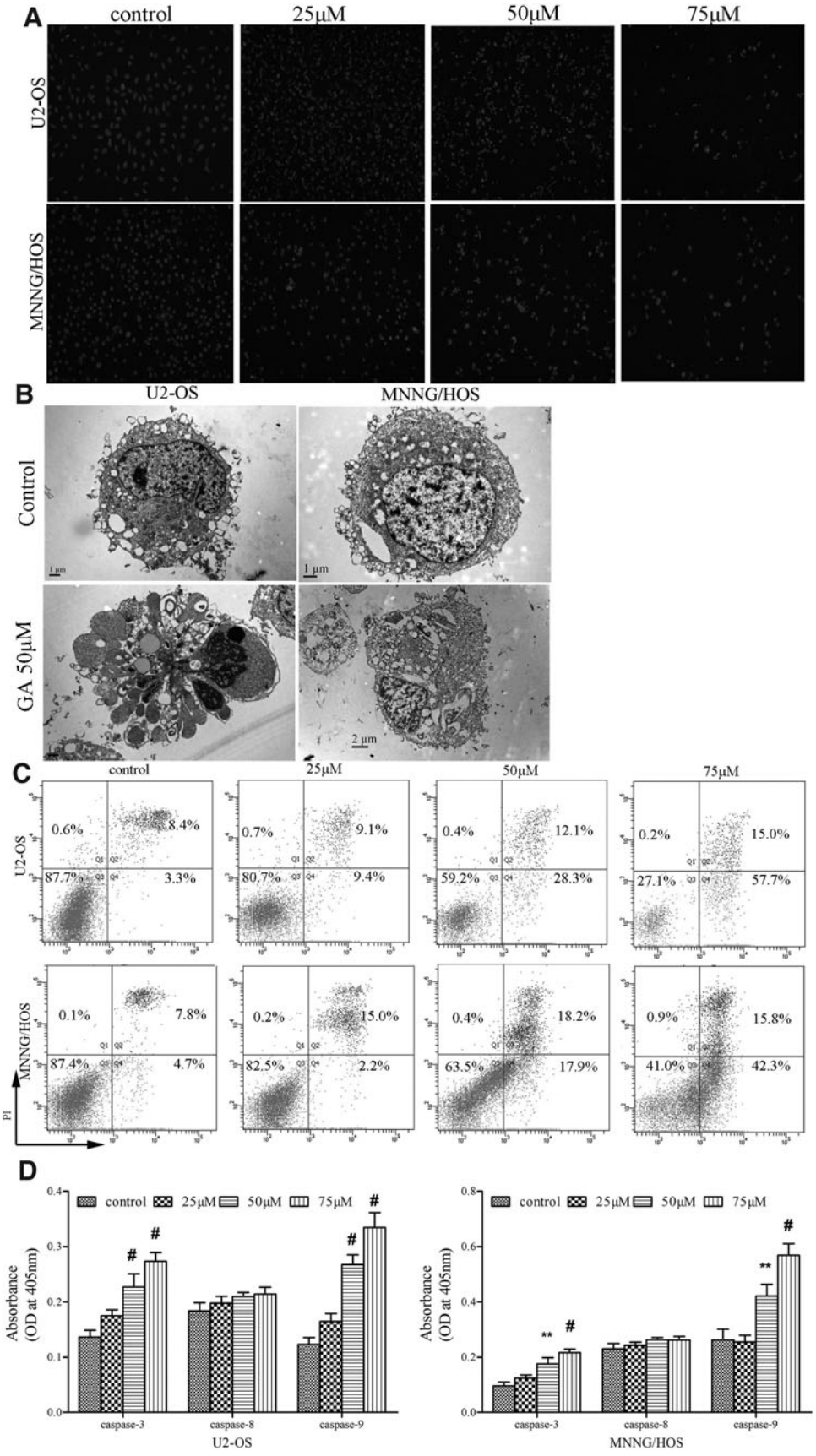

FIG. 2. GA induces apoptosis of human osteosarcoma cells. **(A)** Hoechst staining of osteosarcoma cells treated with 25, 50, and 75 μM for 24 hours, respectively. The nuclei were stained by Hoechst 33258 and visualized under fluorescence microscope (magnification, 200×; scale bar = 100 μm). **(B)** The apoptotic ultrastructure of osteosarcoma cells treated by GA. The cells were examined under a transmission electron microscope (×3700 power). In the 50 μM GA group, typical apoptotic cells were observed in U-2OS and MNNG/HOS; scale bar = 2 μm. **(C)** Annexin V-FITC/PI staining of osteosarcoma cells treated by GA. (a) control group; (b) 25 μM GA; (c) 50 μM GA; (d) 75 μM GA. The data were representative of three independent experiments. **(D)** GA induces the activation of caspase-3 and -9 while does not significantly influence the activation of caspase-8. Lysate was prepared from cells grown in the absence or presence of GA (25, 50, and 75 μM) for 24 hours and tested for activities. Data represented the mean of three measurements ± SD. $^{**}p < 0.01$ versus control group; $^{\#}p < 0.001$ versus control group.

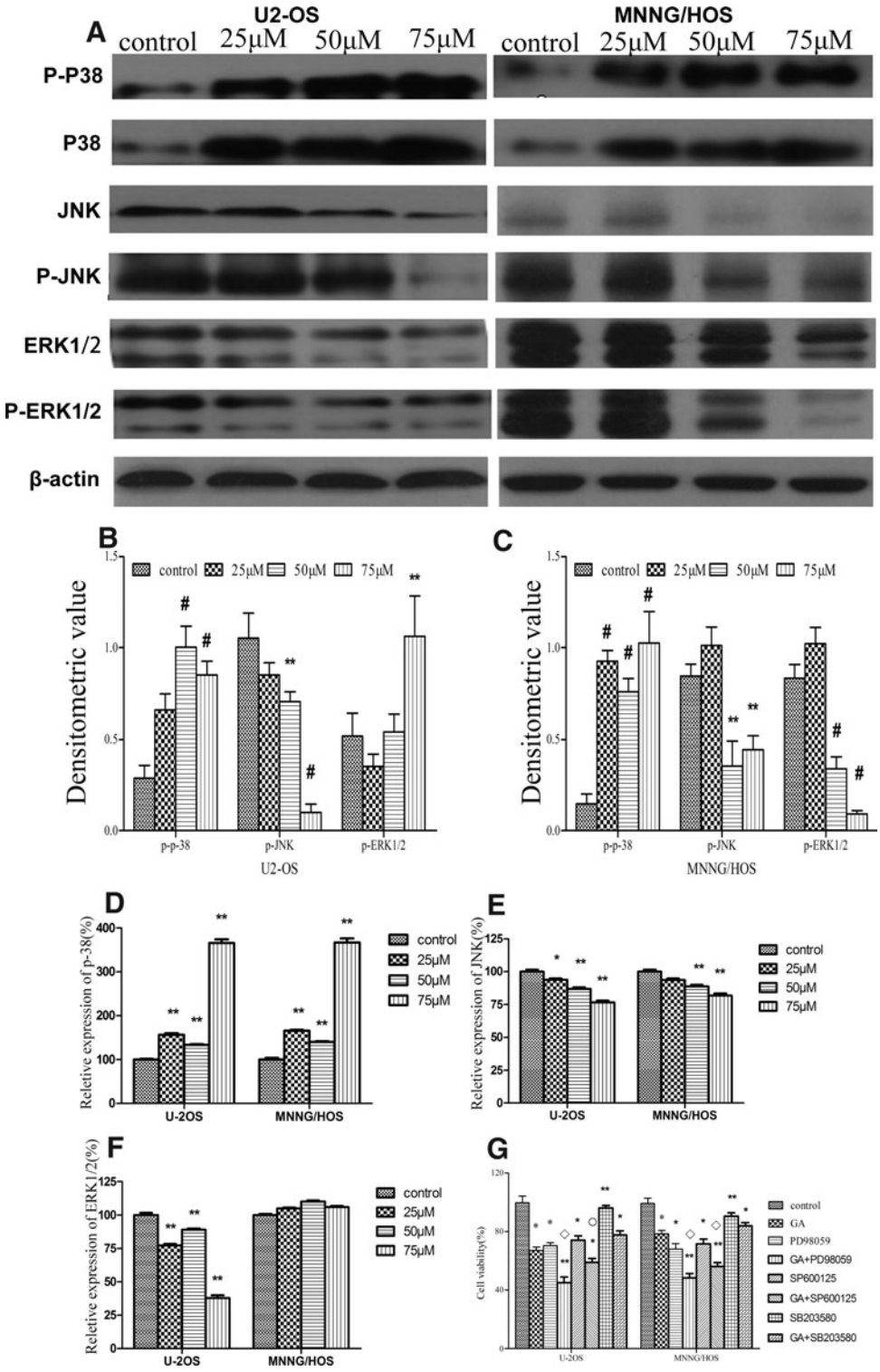

FIG. 3. GA upregulates p-38 activation and downregulates JNK and ERK1/2 activation in human osteosarcoma cells in a dose-dependent manner. **(A–C)** Western blotting analysis of p-38 and p-p-38, JNK and p-JNK, ERK1/2, and p-ERK1/2 in human osteosarcoma cells treated with 25, 50, and 75 μM GA for 24 hours, respectively. The density of target proteins was analyzed by Gel-Pro-analyzer (Media Cybernetics). β-Actin served as loading control. **(D–F)** Real-time RT-PCR analysis for quantitative evaluation of the mRNA expression of target genes. **(G)** The effects of p38, JNK, and ERK1/2 MAPK inhibitors on GA-induced growth inhibition. Data were expressed as mean ± SD of three samples. $^{*}p < 0.05$ versus control group; $^{**}p < 0.01$ versus control group; $^{\#}p < 0.001$ versus control group. $^{\bigcirc}p < 0.05$ GA group versus MAPK inhibitors group. $^{\square}p < 0.01$ GA group versus MAPK inhibitors group. JNK, c-Jun N-terminal kinase; ERK1/2, extracellular signal regulated kinase; MAPK, mitogen-activated protein kinase.

proteins were negatively or positively correlated with GA concentration (Fig. 3B, C). qRT-PCR analysis further showed that the mRNA expression level of p38 kinase was obviously increased after exposure to GA in two cell lines in a dose-dependent manner (Fig. 3D). Moreover, GA decreased JNK kinase mRNA expression in two cell lines (Fig. 3E). Most importantly, mRNA expression level of ERK1/2 kinase decreased in U2-OS cells, while mRNA expression level of ERK1/2 kinase increased in MNNG/HOS cells (Fig. 3F). Taken together, these results suggest that GA may induce apoptosis of human osteosarcoma cells through the inactivation of JNK and ERK1/2 kinase pathways and the activation of p38 kinase pathway.

Next, we employed ERK1/2, JNK, and p38 inhibitors to confirm the role of these signaling pathways in GA-induced apoptosis of osteosarcoma cells. The results showed

that preincubation with PD98059 or SP600125 enhanced growth inhibition induced by GA (from 32.9% ± 2.22% to 54.95% ± 3.98% and from 32.9% ± 2.22% to 41.02% ± 2.73% in U2-OS, and from 21.52% ± 2.40% to 51.63% ± 2.94% and from 21.52% ± 2.40% to 43.88% ± 2.72% in MNNG/HOS, respectively) (Fig. 3G). In contrast, preincubation with p38 inhibitor SB203580 partly blocked GA-induced growth inhibition (from 32.9% ± 2.22% to 22.33% ± 2.92% in U2-OS, and from 21.52% ± 2.40% to 16.10% ± 2.16% in MNNG/HOS, respectively) (Fig. 3G). These data confirm that ERK1/2 and JNK negatively regulate while p38 positively regulates GA-induced apoptosis of osteosarcoma cells.

GA inhibits osteosarcoma in vivo

Finally, we examined the antitumor activity of GA against osteosarcoma *in vivo*. The results showed that GA at dose of 0.3% and 1% dose both inhibited MNNG/HOS tumor xenograft growth in a time-dependent fashion (Fig. 4A). At the end of the experimental period, in average, GA reduced the tumor volume from 2392.99 mm^3 in control group to 1896.34 mm^3 ($p = 0.028$) and 1476.55 mm^3 ($p = 0.0001$) in 0.3% and 1% GA-fed group, respectively (Fig. 4A). However, water intake and gain in body weights did not differ significantly among the control and GA-fed groups during the 6 weeks of experimental period (data not shown). In addition, no mouse died during treatment with either compound or from control group until the end of the experiments (data not shown). Moreover, the toxicity to the mice of GA in the present study is consistent with previous reports.[26,27]

Further histological examination of tumor tissue from vehicle mice showed disorganized arrangement of sarcoma cells and a high cell density. The osteosarcoma cells were ovoid or round and displayed increased ratios of nucleus to cytoplasm. Nuclei were dark and showed clear signs of heteromorphism. In contrast, in tumor tissues from animals treated with GA, the ratio of nucleus to cytoplasm was reduced and the nuclei were polygonal and lightly stained. Nucleoli were small and inconspicuous. The sarcoma cells were loosely arranged and there were marked signs of widespread tumor destruction (Fig. 4B).

In addition, the expression of PCNA and CD31 in GA-treated tumors was evaluated by immunohistochemistry. Qualitative analysis of stained tumor sections revealed that the mean intensity for PCNA decreased from 0.0823 ± 0.0091 in control group to 0.0227 ± 0.0062 and 0.0038 ± 0.0027 ($p < 0.001$) in 0.3% and 1% GA-fed groups, respectively (Fig. 4D, G). Similarly, the mean intensity for CD31 decreased from 0.0432 ± 0.0081 in control group to 0.0316 ± 0.0032 and 0.0173 ± 0.0059 ($p < 0.001$) in 0.3% and 1% GA-treated tumors, respectively (Fig. 4E, H). Moreover, we examined the pro-apoptotic effects of GA under *in vivo* conditions and found that the mean intensity for TUNEL-positive cells significantly increased from 0.0002 ± 0.0001 in tumor sections from control group to 0.0233 ± 0.0023 and 0.0330 ± 0.0045 ($p < 0.001$) in 0.3 and 1% GA-fed groups, respectively (Fig. 4C, F). Collectively, these *in vivo* findings complement the *in vitro* data and suggest that GA exhibits *in vivo* efficacy in inhibiting osteosarcoma by decreasing proliferation, inhibiting angiogenesis, and promoting apoptosis.

Discussion

Osteosarcoma is an aggressive neoplasm representing the most common primary malignant bone tumor.[28] In the past decade, the survival of patients with osteosarcoma has increased, due to rapid advances in neoadjuvant chemotherapy. However, these bone tumors are characterized by frequent metastasis and strong resistance to chemotherapy, and the effectiveness of cytotoxic drugs often declines due to acquired chemoresistance.[1] Finding new therapeutic agents to target the malignant behavior of osteosarcoma cells is therefore important.

Many phytochemicals have been shown to exhibit anticancer efficacy in various *in vitro and in vivo* models of cancer.[29] Among them, GA has been identified as the major active fraction in herbal medicinal plants with growth-inhibitory effect on various cancer cell lines.[27,30–32] In this study, we confirm the anticancer effects of GA on two human osteosarcoma cell lines *in vitro and in vivo*. We found that GA induced apoptosis of human osteosarcoma cells dose and time dependently. The IC_{50} values for GA were 54.23 μM and 87.12 μM for U2-OS and MNNG/HOS cells, respectively. These values differ from those reported for human glioma cells, lung cancer cells, prostate cancer cells, human melanoma, and hepatoma, probably due to the differences in the cell types studied, and the genetic alterations in the cells.[25,27,30,31,33]

Anticancer drugs are known to induce apoptosis, eliminating cells that harbor genetic damage or divide inappropriately.[34] To elucidate the mechanisms of the anticancer actions of GA, we first investigated its pro-apoptotic properties. Annexin V-FITC/PI double staining showed that GA induced apoptosis in a dose-dependent manner in the range of 25–75 μM. Apoptotic cells were further confirmed using fluorescence and electron microscopy. These results are consistent with those reported in other cancer cells.[27,30,31] However, we observed that GA had no effect on osteosarcoma cell cycle, which is different from previous reports in prostate cancer cells.[35]

Activation of caspase-9 and -8 suggests the involvement of both intrinsic and extrinsic pathways of apoptosis that culminates in the activation of caspase-3.[36] Therefore, we determined the role of major caspases in apoptotic death induced by GA. We found that GA caused dose-dependent activation of caspase-3 and -9 by two- to threefolds, but no obvious increase in caspase-8 activity. These findings indicate that GA induces apoptosis in human osteosarcoma cells by activating intrinsic apoptotic pathways.

Members of the MAPK family are important regulators of stress responses, including the induction of apoptosis.[37] Several studies have suggested that p38, JNK, and ERK1/2 cascades have a critical role in the induction of apoptosis.[38,39] Therefore, to elucidate the mechanisms underlying GA-induced apoptosis, the level of p38, p-p38, JNK, p-JNK, ERK1/2, and p-ERK1/2 was analyzed by Western blotting in U2-OS and MNNG/HOS cells. The activation of p38 as indicated by increased p-p38 level was upregulated by GA in both cell lines, while p-ERK1/2 and p-JNK levels were suppressed by GA. These results suggest that GA may inhibit the growth of human osteosarcoma cells by inducing p38 activation and suppressing JNK and ERK1/2 activation.

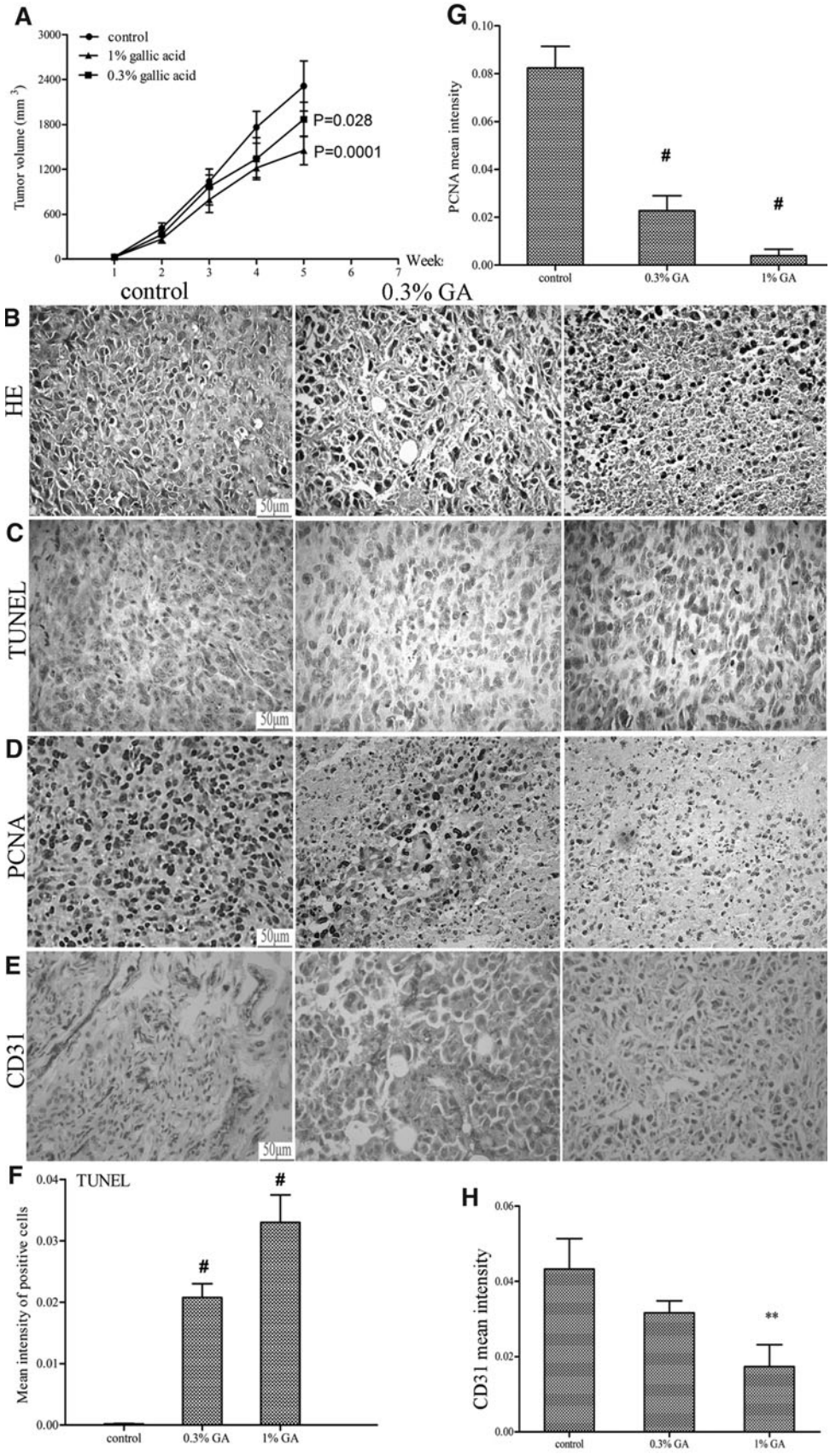

FIG. 4. GA inhibits the growth of MNNG/HOS xenograft in athymic nude mice. Approximately 5×10^6 MNNG/HOS cells were injected subcutaneously into the right axillary fossa of each nude mouse under aseptic conditions. After 24 hours, mice were fed plain water (control group) or 0.3% and 1% (w/v) dose of GA in water for 5 days/week for 5 weeks. **(A)** Average tumor volume (mm^3) was plotted as a function of week of GA feeding. At the end of 5 weeks of xenograft studies, tumors were excised and processed for H&E analysis **(B)** and immunohistochemical staining for TUNEL **(C)**, PCNA **(D)**, and CD31 **(E)**. The representative pictures were taken at $400\times$ magnification of microscopic field from each group. Bar diagrams represented quantitative analysis (mean area ± SD) of TUNEL **(F)**, PCNA **(G)**, and CD31 **(H)** positive cells. Data were shown as mean ± SD. $^{**}p < 0.01$ versus control group; $^{\#}p < 0.001$ versus control group. Scale bar = 50 μm.

Next, we employed special inhibitors of MAPKs and found that GA-induced growth inhibition was almost counteracted by pretreatment with p38 MAPK inhibitor, which was consistent with other reports on an isomycin-induced macrophage death[40] and pyrogallol-induced CPAEC death.[41] Moreover, inhibition of p38 MAPK alone in the absence of GA did not significantly alter cell growth in osteosarcoma cells. However, inhibition of JNK or ERK1/2 signaling led to significant increases in osteosarcoma cell viability after GA treatment, which was also previously found in Hela cells.[8] Therefore, the inhibition of p38 signaling by its inhibitor seemed to antagonize GA-induced apoptosis of osteosarcoma cells, while the inhibition of JNK or ERK1/2 by its inhibitor seemed to exhibit a proapoptosis function. Based on these findings, we conclude that p38, JNK, and ERK1/2 MAPK are all involved in regulating GA-induced growth inhibition of osteosarcoma cells.

In our *in vivo* study, we found that both 0.3% and 1% GA (w/v) obviously inhibited tumor growth during the 5-week treatment period. Histological and ultrastructural analysis of the tumors from mice treated with GA revealed morphological features characteristic of apoptotic cells, in agreement with our *in vitro* findings. Further, the anti-osteosarcoma effect of GA was accompanied by strong anti-proliferative and proapoptotic effects as observed by immunohistochemical analyses of human osteosarcoma xenograft samples for PCNA- and TUNEL-positive cells. Another important aspect of tumor growth and metastasis is angiogenesis, especially for osteosarcoma. In our study, we found that compared with tumors from plain water-fed groups tumors harvested from GA-treated groups had significantly less staining for CD31, a marker for tumor angiogenesis. The anti-angiogenic activity of GA was also shown in previous report.[27] Although subcutaneous grafting is easy to administrate and measure the tumor, the perfect *in vivo* model for bone tumor is the orthotopic transplantation. Therefore, further study employing this model will be more valuable to assess the therapeutic effects of GA on human osteosarcoma.

In summary, in this study we demonstrate the strong anti-osteosarcoma efficacy of GA that is mediated by the modulation of cell proliferation, apoptosis, and angiogenesis. Our findings suggest that GA could be a potent agent for osteosarcoma intervention.

Authors' Contributions

All authors participated in the design, interpretation of the studies, and analysis of the data and review of the article; C.Z.L., H.L., X.P.Z., and H.M.T. conducted the experiments, C.Z.L., Y.Q.T., Z.L.S., and Z.R.Y. performed the statistical analysis and drafted the article; C.Z.L., X.Z., and L.J.T. carried out the computer programming; and H.M.T. supervised the study. All authors read and approved the final article.

Acknowledgments

This study was partly supported by grants from the Natural Science Foundation of Zhejiang Province (No. Y206257), the Science and Technology Planning Project of Zhejiang Province (No. 2009C33093), and the National Nature Science Foundation of China (No. 81171756).

Disclosure Statement

No competing financial interests exist.

References

1. Marina N, Gebhardt M, Teot L, et al. Biology and therapeutic advances for pediatric osteosarcoma. Oncologist 2004;9:422.
2. Entz-Werle N, Choquet P, Neuville A, et al. Targeted apc;twist double-mutant mice: A new model of spontaneous osteosarcoma that mimics the human disease. Transl Oncol 2010;3:344.
3. Liang C, Li H, Shen C, et al. Genistein potentiates the anticancer effects of gemcitabine in human osteosarcoma via the downregulation of Akt and nuclear factor-kappaB pathway. Anticancer Agents Med Chem 2012;12:554.
4. Spencer SL, Sorger PK. Measuring and modeling apoptosis in single cells. Cell 2011;144:926.
5. Genestra M. Oxyl radicals, redox-sensitive signalling cascades and antioxidants. Cell Signal 2007;19:1807.
6. Wagner EF, Nebreda AR. Signal integration by JNK and p38 MAPK pathways in cancer development. Nat Rev Cancer 2009;9:537.
7. Park WH. MAPK inhibitors differentially affect gallic acid-induced human pulmonary fibroblast cell growth inhibition. Mol Med Report 2011;4:193.
8. You BR, Park WH. The effects of mitogen-activated protein kinase inhibitors or small interfering RNAs on gallic acid-induced HeLa cell death in relation to reactive oxygen species and glutathione. J Agric Food Chem 2011;59:763.
9. Chen YC, Chang CN, Hsu HC, et al. Sennoside B inhibits PDGF receptor signaling and cell proliferation induced by PDGF-BB in human osteosarcoma cells. Life Sci 2009;84:915.
10. Noh K, Kim KO, Patel NR, et al. Targeting inflammatory kinase as an adjuvant treatment for osteosarcomas. J Bone Joint Surg Am 2011;93:723.
11. Manna SK, Kuo MT, Aggarwal BB. Overexpression of gamma-glutamylcysteine synthetase suppresses tumor necrosis factor-induced apoptosis and activation of nuclear transcription factor-kappa B and activator protein-1. Oncogene 1999;18:4371.
12. Li L, Ng TB, Gao W, et al. Antioxidant activity of gallic acid from rose flowers in senescence accelerated mice. Life Sci 2005;77:230.
13. Cai Y, Luo Q, Sun M, et al. Antioxidant activity and phenolic compounds of 112 traditional Chinese medicinal plants associated with anticancer. Life Sci 2004;74:2157.
14. Klein E, Weber N. *In vitro* test for the effectiveness of antioxidants as inhibitors of thiyl radical-induced reactions with unsaturated fatty acids. J Agric Food Chem 2001;49:1224.
15. Fiuza SM, Gomes C, Teixeira LJ, et al. Phenolic acid derivatives with potential anticancer properties—a structure-activity relationship study. Part 1: Methyl, propyl and octyl esters of caffeic and gallic acids. Bioorg Med Chem 2004; 12:3581.
16. Zhang J, Li L, Kim SH, et al. Anti-cancer, anti-diabetic and other pharmacologic and biological activities of penta-galloyl-glucose. Pharm Res 2009;26:2066.
17. Lo C, Lai TY, Yang JS, et al. Gallic acid inhibits the migration and invasion of A375.S2 human melanoma cells through the inhibition of matrix metalloproteinase-2 and Ras. Melanoma Res 2011;21:267.
18. Liu KC, Huang AC, Wu PP, et al. Gallic acid suppresses the migration and invasion of PC-3 human prostate cancer cells via inhibition of matrix metalloproteinase-2 and -9 signaling pathways. Oncol Rep 2011;26:177.
19. Hsu JD, Kao SH, Ou TT, et al. Gallic acid induces G2/M phase arrest of breast cancer cell MCF-7 through stabilization

of p27(Kip1) attributed to disruption of p27(Kip1)/Skp2 complex. J Agric Food Chem 2011;59:1996.
20. Ou TT, Wang CJ, Lee YS, et al. Gallic acid induces G2/M phase cell cycle arrest via regulating 14-3-3beta release from Cdc25C and Chk2 activation in human bladder transitional carcinoma cells. Mol Nutr Food Res 2010;54:1781.
21. Liao CL, Lai KC, Huang AC, et al. Gallic acid inhibits migration and invasion in human osteosarcoma U-2 OS cells through suppressing the matrix metalloproteinase-2/-9, protein kinase B (PKB) and PKC signaling pathways. Food Chem Toxicol 2012;50:1734.
22. Liang CZ, Zhang JK, Shi Z, et al. Matrine induces caspase-dependent apoptosis in human osteosarcoma cells *in vitro* and *in vivo* through the upregulation of Bax and Fas/FasL and downregulation of Bcl-2. Cancer Chemother Pharmacol 2012;69:317.
23. Xavier LL, Viola GG, Ferraz AC, et al. A simple and fast densitometric method for the analysis of tyrosine hydroxylase immunoreactivity in the substantia nigra pars compacta and in the ventral tegmental area. Brain Res Brain Res Protoc 2005;16:58.
24. Ji BC, Hsu WH, Yang JS, et al. Gallic acid induces apoptosis via caspase-3 and mitochondrion-dependent pathways *in vitro* and suppresses lung xenograft tumor growth *in vivo*. J Agric Food Chem 2009;57:7596–7604.
25. Lo C, Lai TY, Yang JH, et al. Gallic acid induces apoptosis in A375.S2 human melanoma cells through caspase-dependent and -independent pathways. Int J Oncol 2010;37:377.
26. Raina K, Rajamanickam S, Deep G, et al. Chemopreventive effects of oral gallic acid feeding on tumor growth and progression in TRAMP mice. Mol Cancer Ther 2008;7:1258.
27. Kaur M, Velmurugan B, Rajamanickam S, et al. Gallic acid, an active constituent of grape seed extract, exhibits anti-proliferative, pro-apoptotic and anti-tumorigenic effects against prostate carcinoma xenograft growth in nude mice. Pharm Res 2009;26:2133.
28. Picci P. Osteosarcoma (osteogenic sarcoma). Orphanet J Rare Dis 2007;2:6.
29. Nishino H, Satomi Y, Tokuda H, et al. Cancer control by phytochemicals. Curr Pharm Des 2007;13:3394.
30. Lu Y, Jiang F, Jiang H, et al. Gallic acid suppresses cell viability, proliferation, invasion and angiogenesis in human glioma cells. Eur J Pharmacol 2010;641:102.
31. Choi KC, Lee YH, Jung MG, et al. Gallic acid suppresses lipopolysaccharide-induced nuclear factor-kappaB signaling by preventing RelA acetylation in A549 lung cancer cells. Mol Cancer Res 2009;7:2011.
32. Chen HM, Wu YC, Chia YC, et al. Gallic acid, a major component of Toona sinensis leaf extracts, contains a ROS-mediated anti-cancer activity in human prostate cancer cells. Cancer Lett 2009;286:161.
33. Jagan S, Ramakrishnan G, Anandakumar P, et al. Antiproliferative potential of gallic acid against diethylnitrosamine-induced rat hepatocellular carcinoma. Mol Cell Biochem 2008;319:51.
34. Qazi A, Pal J, Maitah M, et al. Anticancer activity of a broccoli derivative, sulforaphane, in barrett adenocarcinoma: Potential use in chemoprevention and as adjuvant in chemotherapy. Transl Oncol 2010;3:389.
35. Agarwal C, Tyagi A, Agarwal R. Gallic acid causes inactivating phosphorylation of cdc25A/cdc25C-cdc2 via ATM-Chk2 activation, leading to cell cycle arrest, and induces apoptosis in human prostate carcinoma DU145 cells. Mol Cancer Ther 2006;5:3294.
36. Hartojo W, Silvers AL, Thomas DG, et al. Curcumin promotes apoptosis, increases chemosensitivity, and inhibits nuclear factor kappaB in esophageal adenocarcinoma. Transl Oncol 2010;3:99.
37. Johnson GL, Lapadat R. Mitogen-activated protein kinase pathways mediated by ERK, JNK, and p38 protein kinases. Science 2002;298:1911.
38. Tournier C, Hess P, Yang DD, et al. Requirement of JNK for stress-induced activation of the cytochrome c-mediated death pathway. Science 2000;288:870.
39. Kim BM, Chung HW. Desferrioxamine (DFX) induces apoptosis through the p38-caspase8-Bid-Bax pathway in PHA-stimulated human lymphocytes. Toxicol Appl Pharmacol 2008;228:24.
40. Croons V, Martinet W, Herman AG, et al. The protein synthesis inhibitor anisomycin induces macrophage apoptosis in rabbit atherosclerotic plaques through p38 mitogen-activated protein kinase. J Pharmacol Exp Ther 2009;329:856.
41. Han YH, Moon HJ, You BR, et al. JNK and p38 inhibitors increase and decrease apoptosis, respectively, in pyrogallol-treated calf pulmonary arterial endothelial cells. Int J Mol Med 2009;24:717.